J|A|C|S
ARTICLES
Published on Web 01/19/2006

Application of Badger's Rule to Heme and Non-Heme Iron−Oxygen Bonds: An Examination of Ferryl Protonation States

Michael T. Green

Contribution from the Department of Chemistry, The Pennsylvania State University, University Park, Pennsylvania 16802

Received June 20, 2005; E-mail: mtg10@psu.edu

Abstract: To gain insight into the protonation state of enzymatic ferryl species we have examined the applicability of Badger's rule to heme and non-heme iron−oxygen bonds. Using density functional theory we have calculated r_e and ν_e for the Fe−O bonds of complexes with different axial ligands, iron-oxidation, oxygen-protonation, and spin states. Our results indicate that Badger's rule holds for heme and non-heme oxo and hydroxo complexes. We find that the long Fe−O bonds that have been reported in the crystal structures of the ferryl forms of myoglobin, horseradish peroxidase, cytochrome *c* peroxidase, and catalase deviate substantially from the values predicted by Badger's rule, while the short Fe−O bonds obtained from X-ray absorption measurements are in good agreement with Badger's rule. In light of our analysis we conclude that the ferryl forms of myoglobin, horseradish peroxidase, and cytochrome c peroxidase are authentic iron(IV)oxos with Fe−O bonds on the order of 1.66 Å and pKa's < 4.

Introduction

The iron(IV)oxo (ferryl) species in the thiolate-ligated heme enzyme chloroperoxidase has been reported to be protonated at pH 6.5. X-ray absorption spectroscopy reveals an Fe−O bond of 1.82 Å for this intermediate,[1] a value that is longer than expected for an authentic ferryl unit (typically near 1.65 Å) but in excellent agreement with density functional calculations on a protonated ferryl species (Fe(IV)−OH, 1.81 Å).

The importance of this finding lies in the observation that the ability of metal−oxos to abstract hydrogen scales with the strength of the O−H bond formed during H-atom abstraction.[2] In oxidative heme-enzymes the strength of this O−H bond depends on the one-electron reduction potential of compound I (a ferryl-radical species) and the pK_a of the ferryl species, called compound II (eq 1).

$$D(\mathrm{O{-}H}) = 23.06 \times E^0_{\mathrm{cmpd-I}} + 1.37 \times \mathrm{p}K_{\mathrm{a-cmpd-II}} + 57 \pm 2 \text{ (kcal/mol)} \quad (1)$$

This equation highlights the importance of the ferryl pK_a and suggests a role for thiolate-ligation in cytochrome P450, namely to promote hydrogen abstraction (and subsequent hydroxylation) at viable compound I reduction potentials.[1]

Recent crystallographic studies suggest that other enzymatic ferryl species may be protonated as well. The protonation state of these intermediates is inferred from their Fe−O bond lengths, which are longer than expected for an Fe(IV)oxo. Bond lengths of 1.84, 1.92, 1.87, and 1.87 Å have been reported for horseradish peroxidase-II (HRP-II, pH 6.5), myoglobin-II (Mb-II, pH 5.2), cytochrome *c* peroxidase-I (CCP-I, pH 6), and catalase-II (CAT-II, pH 5.2), respectively.[3−6]

X-ray absorption measurements generally paint a different picture. They suggest that HRP-II, Mb-II, and CCP-I are Fe(IV)oxos. Fe−O distances of 1.67 and 1.69 Å have been found for CCP-I (pH 6) and Mb-II (pH *not given*).[7,8] Two independent studies of HRP-II (pH 6−7) have yielded oxo-like bonds of 1.64 and 1.70 Å,[1,9] but a bond of 1.93 Å (pH 7) has also been reported.[10] No EXAFS data has been published for CAT-II.

Fe−O stretching frequencies have been reported for these intermediates. Resonance Raman measurements have provided values of 780 cm^{-1} (pD 4), 753 cm^{-1} (pH 4), 797 cm^{-1} (pH 8.5), and 775 cm^{-1} (pH 7) for HRP-II, CCP-I, Mb-II, and CAT-II, respectively.[11−15] These stretching frequencies are similar to the 790 cm^{-1} (pH 7) stretch found for the Fe(IV)oxo in HRP-I.[16]

(1) Green, M. T.; Dawson, J. H.; Gray, H. B. *Science* **2004**, *304*, 1653−1656.
(2) Mayer, J. M. *Acc. Chem. Res.* **1998**, *31*, 441−450.
(3) Berglund, G. I.; Carlsson, G. H.; Smith, A. T.; Szoke, H.; Henriksen, A.; Hajdu, J. *Nature* **2002**, *417*, 463−468.
(4) Hersleth, H. P.; Dalhus, B.; Gørbitz, C. H.; Andersson, K. K. *J. Biol. Inorg. Chem.* **2002**, *7*, 299−304.
(5) Bonagura, C. A.; Bhaskar, B.; Shimizu, H.; Li, H. Y.; Sundaramoorthy, M.; McRee, D. E.; Goodin, D. B.; Poulos, T. L. *Biochemistry* **2003**, *42*, 5600−5608.
(6) Murshudov, G. N.; Grebenko, A. I.; Brannigan, J. A.; Antson, A. A.; Barynin, V. V.; Dodson, G. G.; Dauter, Z.; Wilson, K. S.; Melik-Adamyan, W. R. *Acta Crystallogr.* **2002**, *D58*, 1972−1982.
(7) Chance, M.; Powers, L.; Poulos, T.; Chance, B. *Biochemistry* **1986**, *25*, 1266−1270.
(8) Chance, M.; Powers, L.; Kumar, C.; Chance, B. *Biochemistry* **1986**, *25*, 1259−1265.
(9) Penner-Hahn, J. E.; Eble, K. S.; McMurry, T. J.; Renner, M.; Balch, A. L.; Groves, J. T.; Dawson, J. H.; Hodgson, K. O. *J. Am. Chem. Soc.* **1986**, *108*, 7819−7825.
(10) Chance, B.; Powers, L.; Ching, Y.; Poulos, T.; Schonbaum, G. R.; Yamazaki, I.; Paul, K. G. *Arch. Biochem. Biophys.* **1984**, *235*, 596−611.
(11) Sitter, A. J.; Reczek, C. M.; Terner, J. *J. Biol. Chem.* **1985**, *260*, 7515−7522.

 10.1021/ja054074s CCC: $33.50

Table 1. Fe−O Bond Lengths, Stretching Frequencies, Spin, and Iron Oxidation States for FeXYPorphyrin

X[a]	Y	oxidation state	spin state	R (Å)	calcd ν (cm^{-1})	scaled ν (cm^{-1})	Badger ν (cm^{-1})
none[b]	O	IV	$S=1$	1.627	944	852	843
thiolate	O	IV[c]	$S=1$	1.634	925	836	829
phenolate	O	IV[d]	$S=1$	1.648	890	804	803
phenolate	O	IV[c]	$S=1$	1.648	878	793	803
imidazole	O	IV[d]	$S=1$	1.652	877	792	795
imidazole	O	IV[c]	$S=1$	1.652	869	785	795
thiolate	O	IV[d]	$S=1$	1.669	835	754	765
imidazole	OH	IV	$S=1$	1.762	682	616	629
phenolate	OH	IV	$S=1$	1.779	665	601	608
imidazole	OH	III	$S=1/2$	1.812	657	594	571
phenolate	OH	III	$S=1/2$	1.814	651	588	569
thiolate	OH	IV	$S=1$	1.813	625	565	570
imidazolate	OH	III	$S=1/2$	1.850	604	546	533
thiolate	OH	III	$S=1/2$	1.852	593	536	531
phenolate	OH	II	$S=0$	1.893	547	494	495
imidazole	OH	II	$S=0$	1.905	540	488	485
thiolate	OH	II	$S=0$	1.920	511	462	473
imidazole	OH_2	III	$S=1/2$	1.998	−	−	
phenolate	OH_2	III	$S=1/2$	2.013	−	−	
thiolate	OH_2	III	$S=1/2$	2.093	−	−	
						average error[e]	9 cm^{-1} (1.4%)

[a] Thiolate = methylthiolate, phenolate = methylguanidinium bound phenolate. [b] FeOTPP. [c] Compound I. [d] Compound II. [e] Badger vs scaled.

For CCP-I and HRP-II the ferryl bond lengths determined by EXAFS measurements and X-ray crystallography are incompatible. The observed ferryl stretching frequencies appear to support the EXAFS results, but it has been argued that the weaker stretch in CCP-I (37 cm^{-1} relative to HRP-I) agrees with the crystallographic assignment of an Fe−O single bond in this intermediate.[5]

The EXAFS data for HRP-II have contributed to the confusion. The ferryl stretching frequency of HRP-II is known to undergo an 11 cm^{-1} red-shift with decreasing pH ($pK_a \approx 8.5$).[17] This red-shift is generally thought to be indicative of the formation of a hydrogen bond to the ferryl oxygen,[11] but the pH-dependent nature of the frequency change and the inconsistent HRP-II EXAFS reports have been used to argue for two pH-dependent (i.e., protonated and unprotonated) forms of HRP-II. As a result of this line of reasoning, similarities in the optical absorption spectra of HRP-II (pH ≤ 7) and Mb-II (pH 3.5) have been used to support the assignment of a long Fe−O bond in the Mb-II crystal structure.[4]

In hopes of clarifying the issue of ferryl protonation, we have examined the applicability of Badger's rule to heme iron−oxygen bonds. Badger's rule is an empirical formula that relates bond distance and vibrational frequency, eq 2[18]

$$r_e = \frac{C_{ij}}{\nu_e^{2/3}} + d_{ij} \qquad (2)$$

where r_e is the equilibrium internuclear distance, ν_e is the vibrational frequency, and C_{ij} and d_{ij} are empirical constants determined for a pair of atoms by fitting a collection of r_e and ν_e.

Badger's rule has been applied with great utility to small polyatomic molecules, but there is no guarantee that a general relationship between bond length and vibrational frequency exists. If the applicability of Badger's rule to Fe−O bonds of heme complexes with different proximal ligands, iron-oxidation, and oxygen-protonation states can be shown, it should provide an excellent tool for discerning the reliability of ferryl bond lengths determined with X-ray structural techniques.

Methods

Using density functional calculations (UB3LYP/6-311G)[19] we determined r_e and ν_e for the 20 heme systems shown in Table 1. In all cases except the ferric-aquo complexes, the Fe−O stretching mode was assigned by an analysis of the normal coordinate potential energy distribution (Supporting Information).[20] The ferric−aquo complexes have a number of low-frequency modes with significant Fe−O vibrational character, making it difficult to assign a definitive Fe−O stretching mode. As a result, ν_{FeO} are not listed for these complexes, and they were not included in our analysis of the applicability of Badger's rule to heme iron−oxygen bonds. The addition of polarization and diffuse functions (6-311+G*) to our basis set had little effect on calculated bond length or vibrational frequency. Calculations on a ferryl porphine using the 6-311G (6-311+G*) basis set yielded an Fe−O bond distance of 1.625 (1.610) Å and an Fe−O vibrational frequency of 947 (944) cm^{-1}.

Calculated frequencies were scaled by 0.903. This value was determined by forcing agreement between the calculated (ν_{FeO} = 944 cm^{-1}) and the experimentally observed (ν_{FeO} = 852 cm^{-1})[21] stretching frequency of an iron(IV)oxo tetraphenylporphyrin (FeOTPP) complex. For the six-coordinate complexes listed in Table 1, a scaling factor of 0.903 results in ferryl stretching frequencies that range from 754 to 836 cm^{-1}. A similar range is observed experimentally for HRP-II, CCP-I, Mb-II, and CAT-II. The 0.903 scaling factor results in an Fe−O stretching frequency of 546 cm^{-1} for an imidazolate-ligated low-spin ferric hydroxide complex, which is in good agreement with resonance

(12) Reczek, C. M.; Sitter, A. J.; Terner, J. *J. Mol. Struct.* **1989**, *214*, 27−41.
(13) A stretching frequency of 767 cm^{-1} has also been assigned to the ferryl unit of CCP-I. Hashimoto, S.; Teraoka, J.; Inubushi, T.; Yonetani, T.; Kitagawa, T. *J. Biol. Chem.* **1986**, *261*, 1110−1118.
(14) Sitter, A. J.; Reczek, C. M.; Terner, J. *Biochim. Biophys. Acta* **1985**, *828*, 229−235.
(15) Chuang, W. J.; Heldt, J.; Van Wart, H. E. *J. Biol. Chem.* **1989**, *264*, 14209−14215.
(16) Kincaid, J. R.; Zheng, Y.; Al-Mustafa, J.; Czarnecki, K. *J. Biol. Chem.* **1996**, *271*, 28805−28811.
(17) The pK_a associated with the shift in ferryl stretching frequency is isozyme dependent. HRP isozymes A-1,2 have $pK_a \approx 6.9$. Isozymes B and C have $pK_a \approx 8.5$.
(18) Badger, R. M. *J. Chem. Phys.* **1935**, *3*, 710−714.
(19) Frisch, M. J. et al. *Gaussian 03*; Gaussian, Inc.: Wallingford CT, 2004.
(20) Painter, P. C.; Coleman, M. M.; Koenig, J. L. *The Theory of Vibrational Spectroscopy and Its Application to Polymeric Materials*. Wiley: New York, 1982.
(21) Shantha, P. K.; Verma, A. L. *Inorg. Chem.* **1996**, *35*, 2723−2725.

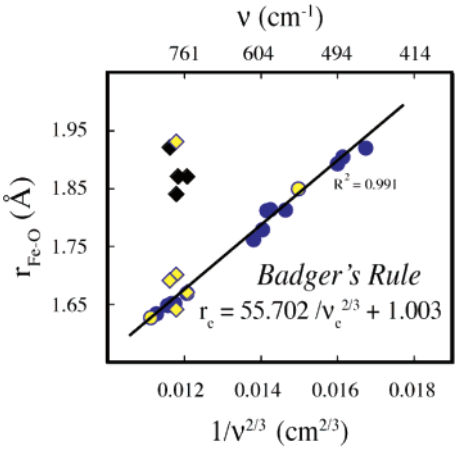

Figure 1. Fe−O bond length versus $1/\nu_{FeO}^{2/3}$. Yellow and blue circles represent calculated bond distances and frequencies (scaled). Yellow circles are points that were used to determine/evaluate the adequacy of the scaling parameter. Best-fit line to theoretical data is given by Badger's rule. Diamonds represent experimental data. Yellow diamonds are from resonance Raman and EXAFS experiments. Black diamonds are from resonance Raman and X-ray crystallography.

Raman measurements on the low-spin ferric hydroxide form of myoglobin (pH 10.4, $\nu_{FeO} = 550$ cm^{-1}).[22] The agreement between theory and experiment in both the high- and low-frequency regions (yellow circles in Figure 1) suggests that the scaling factor of 0.903 is adequate for our purpose.[23]

Results and Discussion

In Figure 1, calculated bond distance is plotted as a function of scaled vibrational frequency (blue and yellow circles). The best-fit line has the form of Badger's rule with the empirical constants $C_{Fe-O} = 55.702$ and $d_{Fe-O} = 1.003$. Also shown in Figure 1 are the points (black diamonds) associated with the experimentally observed Fe−O stretching frequencies and the crystallographically determined Fe−O bond distances for Mb-II, HRP-II, CCP-I, and CAT-II. These values deviate substantially from those predicted by Badger's rule. In contrast, the points associated (yellow diamonds) with the experimentally observed Fe−O stretching frequencies and the EXAFS determined Fe−O bond distances for Mb-II, HRP-II, and CCP-I are in good agreement with the values obtained from our theoretical analysis. The one exception is the minority HRP-II EXAFS report that provided an Fe−O bond of 1.93 Å.

The 753 cm^{-1} Fe−O stretch in CCP-I and the pH-dependent red-shift of ν_{FeO} in HRP-II have been used to argue for the long Fe−O bond in the CCP-I crystal structure ($r_{FeO} = 1.87$ Å) and a protonated form of HRP-II. It is therefore illuminating to use Badger's rule to predict the bond lengths expected for these systems. The Fe−O stretching frequency in CCP-I is 37 cm^{-1} weaker than the $\nu_{FeO} = 790$ cm^{-1} observed for HRP-I. Using Badger's rule one obtains Fe−O bonds of 1.657 and 1.676 Å for HRP-I and CCP-I, respectively, a difference of only 0.019 Å. The Fe−O stretching frequency in HRP-II shifts from 787 to 776 cm^{-1} as the enzyme changes from its alkaline to its acidic form. Badger's rule predicts a change of only 0.006 Å for this transition. These minor variations in bond length can be

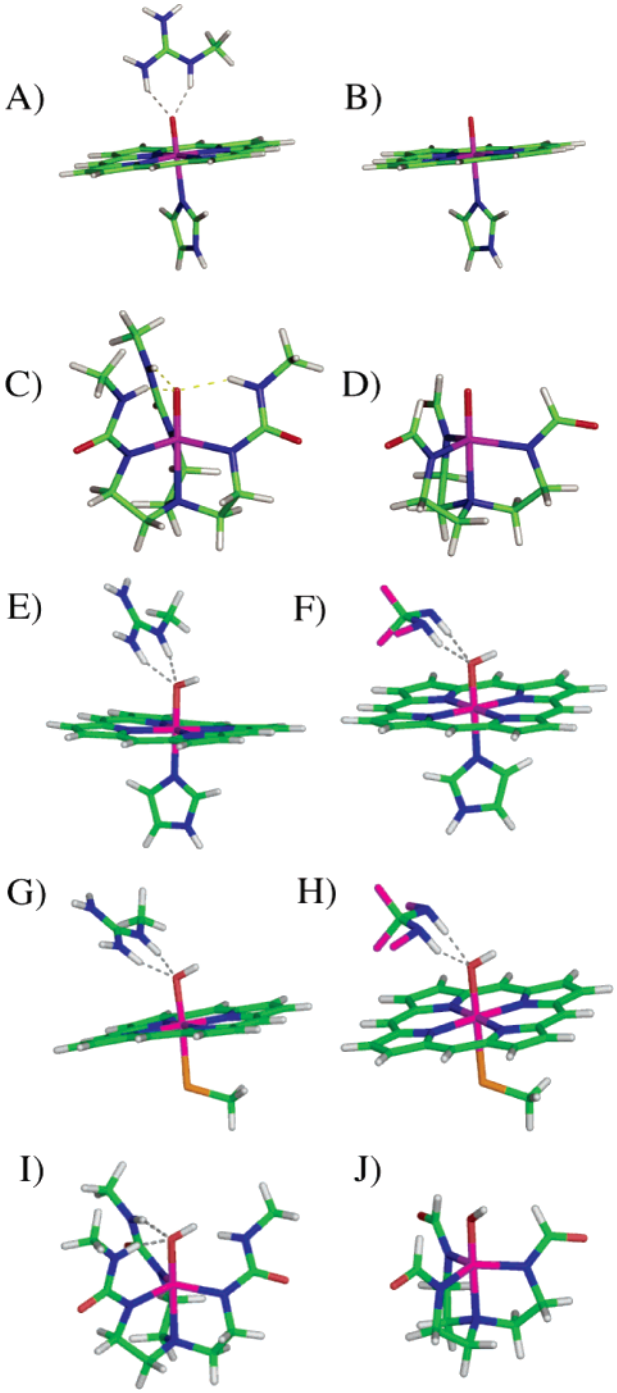

Figure 2. Models used for calculations. Charge of each complex is that required to obtain a formal Fe(IV) oxidation state. (**A**, **B**) Imidazole-ligated ferryl-heme (**A**) with and (**B**) without hydrogen-bonded methylguanidinium cation. (**C**, **D**) Ferryl complexes with variants of Borovik's tripodal tris-[(*N*′-*tert*-butylureaylato)-*N*-ethyl]aminato ($[H_31]^{-3}$) ligand,[25] in which the *tert*-butylimido groups of $[H_31]^{-3}$ have been replaced with (**C**) methylimidos and (**D**) hydrogens. (**E**, **F**) Imidazole-ligated FeOH−porphyrin with hydrogen-bonded (**E**) methylguanidinium cation and (**F**) neutral $CF_2(NFH)_2$. (**G**, **H**) Thiolate-ligated FeOH−porphyrin with hydrogen-bonded (**G**) methylguanidinium cation and (**H**) neutral $CF_2(NFH)_2$. (**I**, **J**) Respective protonated forms of (**C**) and (**D**).

(22) Feis, A.; Marzocchi, M. P.; Paoli, M.; Smulevich, G. *Biochemistry* **1994**, *33*, 4577−4583.

(23) The $\nu_{FeO} = 943$ cm^{-1} and 0.903 scaling factor determined for FeOTPP are similar to the values obtained from a local density functional study of oxo(porphyrinato)iron(IV). Ghosh and co-workers determined an Fe−O stretching frequency of 934 cm^{-1} for the ferryl porphine complex, which requires a scaling factor of 0.912 to obtain agreement with measured values. (Ghosh, A.; Almlöf, J.; Que, L., Jr. *J. Phys. Chem.* **1994**, *98*, 5576−5579.) Our 0.903 scaling factor is also similar to the average scaling (0.914) required to obtain agreement between theory (B3LYP/VDZ) and experiment for the Fe−XO stretch in XO adducts (X = C, N, O) of Fe(II) porphyrins (Vogel, K. M.; Kozlowski, P. M.; Zgierski, M. Z.; Spiro, T. G. *J. Am. Chem. Soc.* **1999**, *121*, 9915−9921).

Table 2. Fe−O Bond Lengths, Stretching Frequencies, Spin and Iron-Oxidation States, Charge, and Implicit Solvation (COSMO)

complex[a]	oxidation state	spin state	charge/ solvation	R_{FeO}(Å)	calcd ν (cm^{-1})	scaled ν (cm^{-1})	Badger ν (cm^{-1})
A	IV	$S=1$	1/none	1.671	868	783	761
B	IV	$S=1$	0/none	1.652	877	792	795
C	IV	$S=2$	−1/none	1.680	830	749	746
C′	III	$S=5/2$	−2/CH_3OH	1.817	653	589	566
FeO[$H_3$1]	III	$S=5/2$	−2/ CH_3OH	1.806	676	610	578
D	IV	$S=2$	−1/none	1.650	907	819	799
D′	III	$S=5/2$	−2/CH_3OH	1.770	737	666	619
E	III	$S=1$	2/none	1.891	550	497	498
F	III	$S=1$	1/none	1.869	582	526	516
G	III	$S=0$	1/none	1.884	538	486	502
H	III	$S=1$	0/none	1.925	498	450	470
I	III	$S=2$	0/none	1.913	529	477	479
I′	III	$S=5/2$	−1/none	1.936	512	462	461
J	IV	$S=2$	0/none	1.768	728	657	621
J′	III	$S=5/2$	−1/none	1.838	641	579	545
						average error[b]	19 cm^{-1} (3.1%)
						heme/non-heme average error[b]	14/22 cm^{-1} (2.5/3.4%)

[a] Reduction of X by one-electron yields X′. [b] Badger vs scaled. **B** was not included in the error analysis, as it was part of the training set.

explained by the presence of hydrogen bonding. CCP-I has two hydrogen bonds (Arg48 and Trp51) to the ferryl oxygen.[5] In HRP-II it is believed that His42 is protonated in the acidic form of the enzyme and that this protonated residue hydrogen-bonds either directly,[11] or via an intervening water molecule,[3] with the ferryl oxygen.

To examine the role that hydrogen bonding plays in modulating Fe−O distances and vibrational frequencies, we examined the heme and non-heme systems shown in Figure 2. To determine the applicability of Badger's rule to these complexes, calculated frequencies were compared with those obtained from the empirical formula, as given in Figure 1. For the 14 previously unexamined compounds listed in Table 2, Badger's rule provides vibrational frequencies with an average error of 19 cm^{-1}. This result strongly suggests that Badger's rule is applicable to the iron−oxygen bonds of our oxo and hydroxo complexes, regardless of oxidation state, spin state, axial-ligation, hydrogen-bonding, solvation, or coordination environment.

Calculations on **A**−**D** reveal that hydrogen bonds have little effect on the Fe−O distances of authentic ferryl species. Two hydrogen-bonding interactions in **A** lengthen the Fe−O bond by 0.019 Å, while the three hydrogen-bonds in **C** lengthen the ferryl bond by 0.030 Å.[24,25] These small changes in bond lengths are accompanied by shifts of 9 and 70 cm^{-1}, respectively in the Fe−O stretching frequency. (Badger's rule predicts $\Delta\nu_{FeO}$ = 34 and 53 cm^{-1}, respectively) Thus, we see that while hydrogen bonding can explain substantial shifts in the ferryl stretching frequency, it cannot explain the long Fe−O bonds in the crystal structures of HRP-II, Mb-II, CCP-I, and CAT-II.

Models **E**−**J** were used to examine the effects of hydrogen bonding to hydroxide complexes. Calculations on these systems reveal a general trend. Strong hydrogen bonding to complexes that would formally be considered Fe(IV)OH (in the absence of hydrogen bonding) results in species that are best described as Fe(III)OH radicals. **E** and **F** have porphyrin radicals. **G** and **H** have sulfur-based radicals, and **I** has an unpaired electron on the tripodal ligand.[26] As a result of the change in oxidation state, hydrogen bonding plays a significant role in determining the Fe−O bond lengths of **E**−**I**. These ferric compounds have Fe−O bonds that range from 1.87 to 1.93 Å and Fe−O stretching frequencies that range from 450 to 526 cm^{-1}. (Badger's rule provides 470−516 cm^{-1}.) It is interesting to note that the range of Fe−O bond lengths displayed by the ferric hydroxide complexes in Tables 1 and 2 is similar to that found in the crystals structures of HRP-II, Mb-II, CCP-I, and CAT-II.

Figure 3 captures the essence of this work. It shows calculated bond distances and their related Badger frequencies plotted versus FeO oxidation and protonation state (black diamonds). The top and bottom rows contain the results of experiments on HRP-II, CCP-I, Mb-II, CAT-II, and the ferryl form of taurine dioxygenase (TauD). The top row gives Fe−O stretching frequencies obtained from resonance Raman experiments (open diamonds). The bottom row gives bond distances obtained from EXAFS measurements (blue diamonds) and X-ray crystallography (red diamonds). The Badger frequency (distance) associated with an experimental distance (frequency) can be read from the opposite axis.

The ellipse in Figure 3 highlights the agreement between theory and spectroscopy. Bond distances and stretching frequencies obtained from EXAFS and resonance Raman measurements are in good agreement with each other. The bond distances obtained from the crystal structures are clear outliers. They are not in agreement with the results of any other technique.

The discrepancy between the Fe−O bond distances determined by spectroscopy and those obtained from crystallography is problematic for CCP-I and HRP-II. In both cases, resonance Raman and EXAFS experiments were performed at the same or a more acidic pH than the crystallization conditions. Thus, protonation of the ferryl moiety or a nearby H-bond donor is not an acceptable solution to the dilemma, and in any case, we

(24) Models C and D contain variants of Borovik's tripodal tris[(*N*′-*tert*-butylureaylato)-*N*-ethyl]aminato ([$H_3$1]$^{-3}$) ligand, in which the *tert*-butylimido groups of [$H_3$1]$^{-3}$ have been replaced with (C) methylimidos and (D) hydrogens.

(25) MacBeth, C. E.; Gupta, R.; Mitchell-Koch, K. R.; Young, V. G.; Lushington, G. H.; Thompson, W. H.; Hendrich, M. P.; Borovik, A. S. *J. Am. Chem. Soc.* **2004**, *126*, 2556−2567.

(26) The location of the radical can be determined from changes in spin density that occur upon oxidation of the ferric complex. Oxidation of the ferric forms of E, F, G, H, and I results in the following changes in ligand spin density: 0.97, 0.97, −1.00, −0.70, −0.75. Thus, these systems are ferric hydroxides with ligand-based radicals. In contrast, J is an authentic Fe(IV) species. Oxidation of the ferric form of J results in a ligand spin density change of only −0.10.

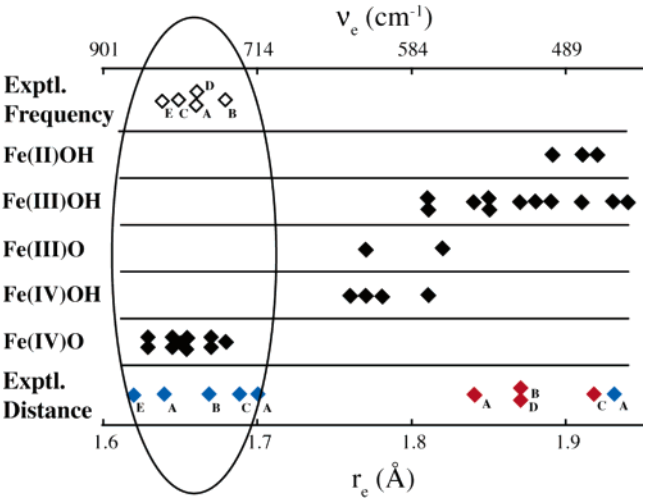

Figure 3. Bottom axis is Fe−O bond distance. Top axis is vibrational frequency obtained by applying Badger's rule as parametrized in Figure 1. Black diamonds represent theoretical results obtained in this paper (i.e. optimized Fe−O distance and ν_e from Badger's rule). The top and bottom rows contain the results of experimental investigations. Open diamonds represent the experimental vibrational frequencies obtained from resonance Raman measurements. Blue and red diamonds represent the bond distances obtained from EXAFS measurements and X-ray crystallography, respectively. Experimental systems are (A) HRP-II, (B) CCP-I, (C) Mb-II, (D) CAT-II, and (E) the ferryl form of TauD. The ellipse highlights the agreement between theory and EXAFS and resonace Raman experiments.

have shown that hydrogen bonding is not a viable mechanism for lengthening a ferryl bond by 0.20 Å.

Figure 3 is compelling. It suggests that either (1) there is a systematic error in the crystallographically determined ferryl bond lengths of ∼0.2 Å, (2) the spectroscopy and crystallography were performed on different forms of the enzyme, or (3) the crystals in question were reduced during data collection. It is difficult to draw other conclusions. The different descriptions of HRP-II and CCP-I provided by spectroscopy and crystallography cannot both be correct. The excellent agreement between theory and resonance Raman and EXAFS spectroscopies suggests that HRP-II and CCP-I are best described as authentic Fe(IV)oxos (i.e., unprotonated ferryls) with Fe−O bonds on the order of 1.66 Å and pK_a's < 4.

The similarities between Mb-II, HRP-II, and CCP-I (all three are imidazole-ligated ferryls) lead us to a similar set of conclusions regarding Mb-II and a similar set of questions concerning the Mb-II crystal structure. A bond of 1.92 Å is *extremely* long for an Fe(IV)−oxygen bond (oxo or hydroxo). Our calculations indicate that imidazole-ligated Fe(IV)−OH porphyrin compexes should have bonds on the order of 1.76 Å. Hydrogen bonding to the FeOH unit can lead to an Fe−O bond of 1.89 Å (Table 2), but the resulting species is best described as an Fe(III)−OH porphyrin radical not an Fe(IV) species. This raises the question: Is the Mb-II crystal reduced? A recent quantum refinement of the Mb-II structure suggests it might be. Quantum refinement is essentially standard crystallographic refinement in which the molecular-mechanics potentials are supplemented by quantum chemical calculations. In theory, one can obtain an accurate description of the protein's active site in various oxidation and protonation states. Then through a comparison of the crystallographic *R*-factors, electron density maps, and strain energies one can determine which of these states best fits the experimental data. Using this technique Nilsson and co-workers found that an Fe(III)−OH description of the active-site provided the best fit to the reported Mb-II structure.[27]

The protonation status of CAT-II is not as clear-cut. CAT-II has a unique axial ligation, making comparisons with HRP, Mb, and CCP questionable. The CAT-II resonance Raman measurements were performed at a more basic pH than the crystallization conditions. Thus, it is possible that the discrepancy between spectroscopy and crystallography could be explained by the protonation of the ferryl moiety.[28,29] EXAFS and resonance Raman measurements of CAT-II at (or below) pH 5.2 would help clarify the issue.

In closing, we return briefly to the thiolate-ligated ferryl in chloroperoxidase. CPO-II has been shown to have an Fe−O bond of 1.82 Å, which suggests protonation of the ferryl moiety. This would explain the absence of a resonance Raman signal attributable to Fe(IV)O stretching in CPO-II; although Kitagawa and co-workers generated the intermediate with the use of $H_2{}^{18}O_2$ and $H_2{}^{18}O$, they could not observe an Fe(IV)O feature in the 655−875 cm^{-1} region, where the vibrational signature of authentic ferryl species appear. Our Badger's rule analysis predicts that the Fe(IV)−OH stretch of CPO-II will be visible near 563 cm^{-1}.

Acknowledgment. Supported by the National Science Foundation, the Petroleum Research Fund, and the Arnold and Mabel Beckman Foundation.

Supporting Information Available: Normal coordinate potential energy distribution and calculated ^{18}O isotopic shifts. This material is available free of charge via the Internet at http://pubs.acs.org.

JA054074S

(27) Nilsson, K.; Hersleth, H. P.; Rod, T. H.; Andersson, K. K.; Ryde, U. *Biophys. J.* **2004**, *87*, 3437−3447.
(28) This possibility was recently examined using a combination of local density functional theory and Car−Parrinello molecular dynamics. The Fe(IV)−O and Fe(IV)−OH bond lengths (1.67 Å and 1.77 Å respectively) obtained with these methods are in good agreement with the values reported in Table 1. Both values are significantly shorter than the 1.86 Å Fe−O bond reported in the crystal structure of CAT-II. The Fe(III)OH form of CAT was not examined.[29]
(29) Rovira, C. *ChemPhysChem* **2005**, *6*, 1820−1826.